Ultrasound wave propagation in glass-bead packing under isotropic compression and uniaxial shear*

Zhi-Gang Zhou(周志刚)[1,2], Yi-Min Jiang(蒋亦民)[3,†], and Mei-Ying Hou(厚美瑛)[1,2,‡]

[1] Key Laboratory of Soft Matter Physics, Beijing National Laboratory for Condense Matter Physics, Institute of Physics, Chinese Academy of Sciences, Beijing 100190, China

[2] University of Chinese Academy of Sciences, Beijing 100049, China

[3] School of Physics and Electronics, Central South University, Changsha 410083, China

(Received 28 March 2017; revised manuscript received 11 April 2017; published online 20 June 2017)

The axial-stress dependence of sound wave velocity in granular packing is experimentally investigated with tri-axial and uni-axial devices. Preparing samples by repetitive loadings and unloadings in a range of 20 kPa–1000 kPa, we find that the axial-stress dependence of sound wave velocity approaches the Hertz scaling with an exponent of 1/6 for large axial stresses (>400 kPa). Weak deviation from the Hertz scaling is seen at low stresses. Repetitive axial loadings slightly reduce this deviation, and sound velocities increase nonlinearly approaching some saturated values. Velocities for uni-axial case are found slightly to be bigger than those for tri-axial isotropic compression case. These effects are discussed in the frameworks of granular solid hydrodynamics (GSH) and effective medium theory (EMT), which indicate that they cannot be explained with density nor Janssen ratio only. Dissipation occurring during wave propagation may be a non-negligible factor.

Keywords: granular materials, ultrasonic wave, Hertz scaling law

PACS: 45.70.–n, 43.25.+y, 83.80.Fg **DOI:** 10.1088/1674-1056/26/8/084502

1. Introduction

The contact law of granular material implies the nonlinear relationship between force F and displacement δ, namely Hertz-law: $F \propto E_0(\delta/d)^{3/2}$, where E_0 is the bulk elastic modulus and d a typical grain diameter.[1] By assuming that microscopic and macroscopic granular displacements remain affine, the "mean-field" Hertz-law gives a scaling between sound velocity and isotropic confining pressure P, i.e., $c \propto c_1(\phi Z)^{1/3}(P/E_0)^{1/6}$, where c_1 is the material bulk velocity, ϕ the packing fraction, and Z the mean number of contact per grain.[2–4] Experimentally, the mean-field relation is only recovered for very high pressure confinement (10^6 Pa for packing of glass spheres); for lower pressure (around 10^5 Pa) the mean-field relation does not hold.[5] Voluminous literature in soil mechanics and geophysics suggests that a scaling for the elastic shear wave velocity — $c \propto P^{1/4}$ — will be more representative of experimental data for pressures ranging from 10^3 Pa to 10^6 Pa.[6,7] Another scaling $c \propto P^{1/3}$ for the elastic shear wave velocity dependence under uniaxial compression is obtained around the jamming transition of a granular packing at the critical point with a critical number of contacts per grain Z_C. These results show contradictory pressure dependence. In this work, we explore the velocity–pressure dependence in glass-bead packing under uniaxial shear and isotropic compression for both longitudinal compression wave and shear wave. A comparison of the pressure dependence measured under rigid wall boundary condition between our experimental results and the results in Ref. [8] is given. We find that within our experimental pressure range (10^4 Pa–10^6 Pa) the elastic shear wave pressure dependence approaches the scaling $c \propto P^{1/6}$ after repetitive axial loadings. Notable deviations are found for low pressure regime (20 kPa–400 kPa). This result indicates that the Hertz scaling holds well for dense repetitive preparation granular sample, at least for the high stress condition when $P > 400$ kPa. Influences of packing density and Janssen ratio (which is different from 1 for the uniaxial case) on the measured velocities are discussed in connection with the mean field and granular solid hydrodynamic (GSH, see Ref. [9]) theories on the assumption that samples are spatially homogeneous and dissipations are negligible. It is found, however, that the influences of packing density and Janssen ratio are small and can be ignored. This indicates that the complicated effects due to dissipations and spatial inhomogeneities may be important for the deviation of the Hertz law in the low stress region.

2. Experiments

Sound propagation in granular material is influenced only by packing fraction and stress status when perturbations of injected waves are small enough. If not, dissipations and plas-

*Project supported by the National Natural Science Foundation of China (Grant Nos. 11274354 and11474326) and the Strategic Priority Research Program-SJ-10 of the Chinese Academy of Sciences (Grant No. XDA04020200).

†Corresponding author. E-mail: jiangyimin@aliyun.com

‡Corresponding author. E-mail: mayhou@iphy.ac.cn

© 2017 Chinese Physical Society and IOP Publishing Ltd

tic deformations may occur during the propagation, of which the influences become complicated and can even be preparation history-dependent. In order to explore the pressure dependence of the wave velocity in granular material we prepare samples under different conditions (Fig. 1). In uniaxial shear experiment we prepare samples as follows: dry glass beads of diameters ranging from 0.8 mm to 1 mm are first poured from a hopper orifice with an 8-mm diameter into a metal cylinder container. We flatten the surface of the sample and seal it up with the ultrasonic transducer on the top. The diameter and height of the container are 51.0 mm and 65.5 mm respectively and the final average packing fraction in the sample is estimated to be around 0.61. The temperature and humidity of experimental environment are kept to be about 26 °C and 40%, respectively.

The ultrasonic transducer with a 50-mm diameter is shown at the top-left corner of Fig. 1(b). It is composed of three parts, i.e., the inner piezoelectric crystal, the metal protection layer and the bender element that generates shear wave. The central frequency of the ultrasonic transducer is 80 kHz, and because the piezoelectric crystal does not directly contact the granular sample, the actual central frequency of sound signal injected into granular sample is less than 80 kHz due to the wave scattering during penetrating the metal protection layer. The axial deformation of the sample is measured by a linear variable differential transformer (LVDT). The effective resolutions of the tri-axial tester are evaluated to be 2.5 kPa for pressure, and 5.0×10^{-6} for the axial strain. Throughout the measurements the axial deformations are found to be small, less than 1.5%.

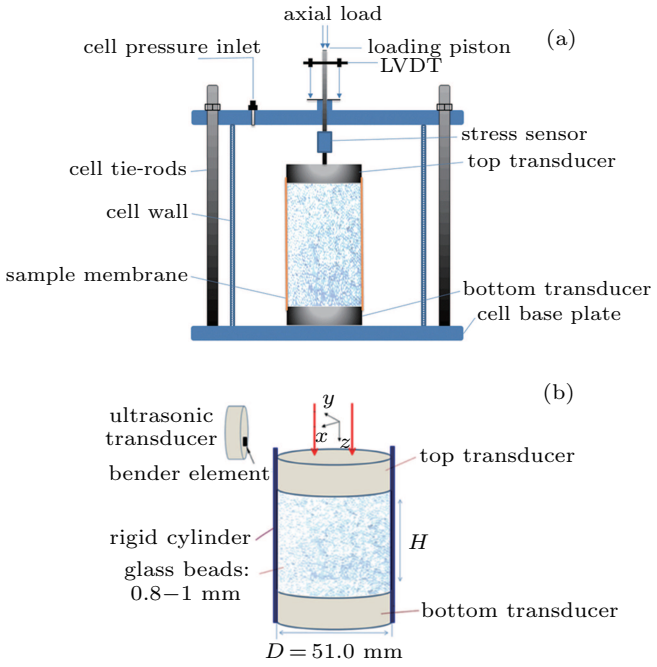


Fig. 1. (color online) Experimental sketches for (a) isotropic compression and (b) uniaxial shear.

In the uni-axial experiments (Fig. 1(b)), the samples are prepared by loading and unloading at the top 15 times. During each loading cycle with load from 20 kPa to 1 MPa, sound velocity and axial deformation are measured in steps of 50 kPa. Velocity is not monitored in the unloading cycle.

The Janssen ratio, defined as $J=\sigma_x/\sigma_z$, is usually different from 1 for samples in the uni-axial experiment, and is a parameter we use to discuss the influence of shear stress. In order to make an estimation, sound velocity in the isotropic compression condition (i.e., $J=1$) is measured using the tri-axial device (Fig. 1(a)). In this case, the sample is enclosed by a thin rubber membrane and confined by water at high-pressures ranging from 20 kPa to 920 kPa controlled by pressure–volume controller (PVC). The sample preparation procedure and the dimensions are the same as those in the uniaxial compression case. As in the uniaxial case, we prepare the sample by repetitive loadings and unloadings of the sample 4 times, while maintaining stress isotropic, i.e., $P=\sigma_x=\sigma_y=\sigma_z$. The stress produced by the rubber membrane itself on the granular sample is estimated to be smaller than 2.5 kPa and thus it is ignored in our experiments. The isotropic measurements are also used to make a comparison with the mean field relation (also known as effective media theory or EMT).

All sound velocities are measured using the time-of-flight method.[5,8,10] Namely we measure the arrival time $\tau_{\rm tof}$ of the front end of the sound wave, and the sound velocity can be obtained by $c=H/\tau_{\rm tof}$, where H is the traveling distance of the wave in the sample.

3. Results and discussion

Assuming that the sample has cylindrical symmetry and wave vector is along its axial direction, the wave can have two components: a longitudinal (also termed P or compression) wave and transverse (also named S or shear) wave. The two sound velocities $c_{\rm L}$ and $c_{\rm T}$ can be generally written as

$$c_{\rm T}=c_0c_\rho c_J\left(\frac{\sigma_z}{P_{\rm atm}}\right)^{1/6}, \tag{1}$$

$$\gamma=\frac{c_T}{c_L}=\gamma_0\gamma_J, \tag{2}$$

where c_ρ and $c_J\gamma_J$ are factors of density and shear, each of which is a function of density ρ and Janssen ratio $J=\sigma_x/\sigma_z$ respectively. They are normalized to 1 at the random loose packing density $\rho_{\rm lp}$ (assume $\rho_{\rm lp}=1394$ kg/m^3) and isotropic stress $J=1$. $P_{\rm atm}$ is the atmosphere pressure. Therefore γ_0 and c_0 respectively represent velocity ratio and S-velocity at the random loose pack density under isotropic atmospheric stress.

If γ_0 and c_0 are kept constant, equations (1) and (2) imply that the factors only influencing the two sound velocities are packing density, Janssen ratio and axial stress, which will be further factorized. Various theories, including both GSH and EMT, support that this is correct when samples are spatially homogeneous, wave amplitudes are small enough such

that dissipations are negligible, and boundary effect can be ignored. However, in real experiments the requirements may be not fully obeyed, deviations of γ_0 and c_0 from constants are often seen. The discussion in the following sections will show that the deviations may unfortunately be comparable to, sometimes even greater than the factors and Hertz 1/6-scaling of Eqs. (1) and (2). As these are main difficulties in examining in detail the relationship between theory and experiment, more experimental investigations on dissipations and non-homogeneity are important and worth performing.

3.1. Sound velocity measurements

The longitudinal and transverse sound velocities measured by the uni-axial and tri-axial devices, with 15 and 4 loading cycles, respectively, are plotted in Fig. 2 as a function of axial stress σ_z. In the figure the measured data reported by Ref. [8] are shown by symbol "*" for comparison. The influence of the loading cycle on the velocity is one of the main focuses of this work. It can be seen that the influence is small for the isotropic tri-axial measurements, but is apparent for the uni-axial case.

Firstly, the velocities of isotropic tri-axial measurements are slightly smaller than those of the uni-axial ones for both P and S waves. As will be discussed in the following subsections, the differences are not likely to be explained with packing density nor Janssen ratio (i.e., the factors c_ρ and $c_J\gamma_J$ in Eqs. (1) and (2)). A possible explanation is to relate the phenomenon to the rigid wall of the container in the uni-axial case. As both the emitter and the detector used in the experiments have the sizes comparable to the sample diameter, the boundary condition (whether rigid or soft membrane) may become a noticeable factor for sound velocity measurements. However, more studies are needed to confirm this in the future.

Secondly, the loading-unloading cycles increase sound velocity systematically and gradually to a saturation limit for both P and S waves. The phenomenon is smaller for isotropic tri-axial measurements, but is apparent for the uni-axial ones. The increase in velocity after repetitive loads can be attributed to the so called "history effect", namely for a newly prepared sample cyclic loads are required to remove unstable shear zones in the bulk or along its boundaries. After the cyclic treatment the sample becomes mechanically more stable.[11] Our experiment suggests that the history effect can be detected and investigated with sound probes.

Thirdly, the log–log plot of the velocities versus axial stress shown in Fig. 2(b) suggests that all data obey the Hertz 1/6-scaling well, especially for larger axial stresses ($\sigma_z >$ 400 kPa). Also a trend of better collapse to the Hertz scaling could be seen after repetitive loads, especially for the case of S-wave curves. The deviation from the Hertz scaling is noticeable at low stresses. This suggests that it is probably due to perturbations of emitted sound waves, of which influences may become stronger for less confined samples under the fixed emitting power used in the present experiment. As mentioned in the Introduction, the problem of deviation from the Hertz scaling has been under debate in literature for quite a long time.[12,13] Clarifying its origin is still a primary concern in the future.

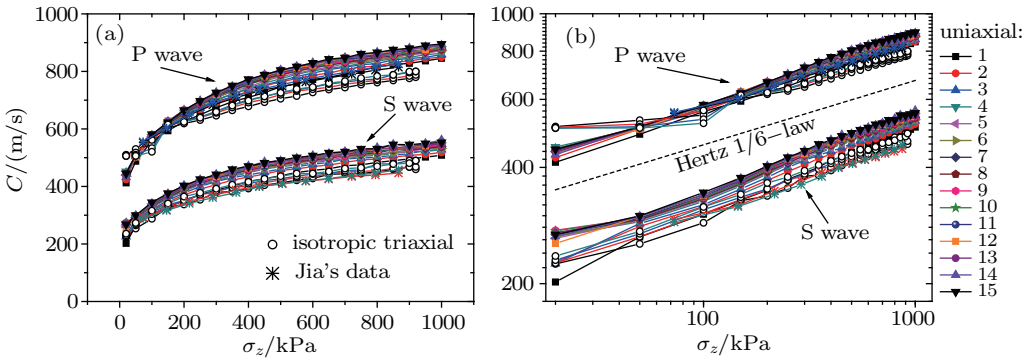


Fig. 2. (color online) Sound velocities measured with isotropic triaxial (black circles) and uniaxial shear (color-filled symbols), in normal (a) and log–log (b) coordinates, as a function of axial stress. Jia's data (*) reported in Ref. [8] are also plotted for comparison.

3.2. Velocity ratio and magnitude

A notable feature of the ratio defined by Eq. (2) is that it is independent of packing density nor axial stress. The γ_0 can be measured directly with the isotropic tri-axial device, for which $\gamma_J = 1$ holds. The results are shown by empty circles in Fig. 3. The obtained γ_0 remains constant for large stress, but remarkable deviations can be seen for low stress, especially when the stress decreases to a level lower than 400 kPa. We consider this as strong evidence that non-equilibrium dissipations are significant in the sound measurement, as all equilibrium influences from density, Janssen ratio, and stress have already been removed in this case. The mechanism of the dissipation is complicated, which is most probably related to inhomogeneous adjustments of grains in the bulk and near the boundary during the wave propagation. It is expected that the influence will become weaker as the wave amplitude decreases. Noting that the dissipations are relatively small in large stresses, we can however obtain γ_0 by averaging those isotropic ratios of

Fig. 3 with $\sigma_z > 400$ kPa. This leads to $\gamma_0 = 0.595$ in our case.

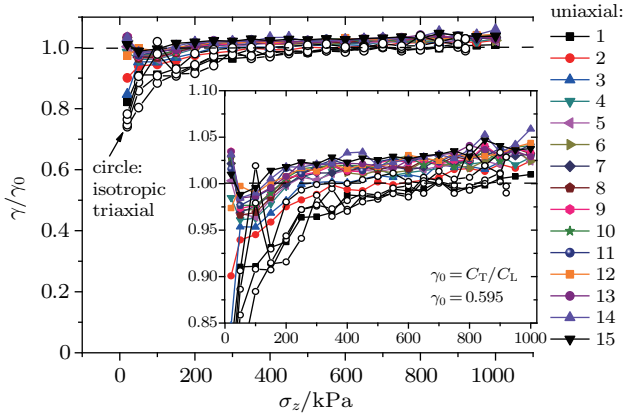


Fig. 3. (color online) Variations of velocity ratio with axial stress for the data shown in Fig. 2, with inset showing magnified main curves.

The velocity ratios of uni-axial data, normalized by the above γ_0, are plotted in Fig. 3 with solid symbols. They are all slightly larger than the isotropic ones, and systematically increase with loading-unloading cycles in a nonlinear manner and approach a certain limit. As the Janssen ratio for silo is widely considered to be less than 1, and the GSH predicts that shear factor $\gamma_J < 1$ for $J < 1$, therefore the observed deviation of γ from γ_0 cannot be explained by the γ_J prediction. A possible cause is the rigid container used in the uni-axial experiment, the interaction of which with glass beads may enhance wave propagations slightly. The effect may be more pronounced for S wave, thus yielding a slightly larger velocity ratio. It is worth noting that the deviation is small (less that 5% for $\sigma_z > 400$ kPa), so more detailed and careful measurements will be needed for clarifying this.

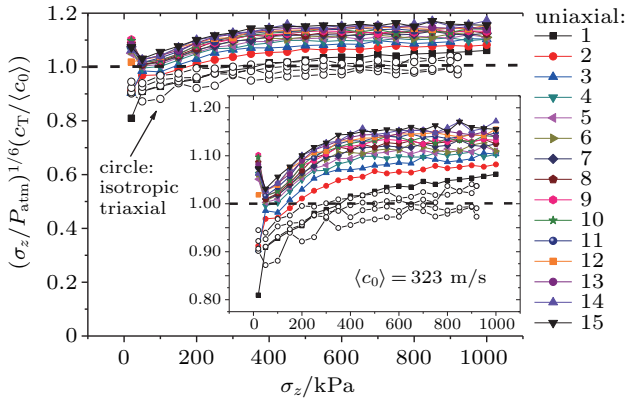


Fig. 4. (color online) Variations of S-velocity with axial stress for the data shown in Fig. 2, with S-velocity normalized by the Hertz scaling and the mean of the isotropic data with $\sigma_z > 400$ kPa. Inset: magnified main curves.

Figure 4 shows the re-plotted measured S-velocities shown in Fig. 2, which are normalized with the Hertz scaling and the mean value $\langle c_0 \rangle = 323$ m/s obtained from averaging the isotropic S-velocities with $\sigma_z > 400$ kPa. Note that the $\langle c_0 \rangle$ is obtained with the packing density of the sample used in this experiment, which may differ from c_0 in Eq. (1) defined with the random loose packing density. It can be seen that for uni-axial case, the variations of S-velocity with the cyclic loads is much greater than those for isotropic case.

Deviation from the Hertz law can be seen in Fig. 4, as the curves are not all strictly horizontal, especially in low stress regime. Other effects connected to the load-unload cycles and difference between uni-axial and isotropic tri-axial measurements, are similar to those discussed above for γ. They are again considered to be mainly caused by the complicated dissipation, inhomogeneity and boundary of the sample.

3.3. Theory

For the case of isotropic stress $\sigma_x = \sigma_z = P$, the EMT predicts the longitudinal and transverse velocities[2,3]

$$c_L = \sqrt{\frac{3K+4\mu}{3\rho}}, \tag{3}$$

$$c_T = \sqrt{\frac{\mu}{\rho}}, \tag{4}$$

where ρ is the mass density of granular sample. The bulk and shear moduli K and μ are given by

$$K = \frac{C_n}{12\pi}(\phi Z)^{3/2}\left(\frac{6\pi P}{C_n}\right)^{1/3}, \tag{5}$$

$$\mu = \frac{C_n + \frac{3}{2}C_t}{20\pi}(\phi Z)^{3/2}\left(\frac{6\pi P}{C_n}\right)^{1/3}. \tag{6}$$

Here, $C_n = 4\mu_g/(1-\nu_g)$ and $C_t = 8\mu_g/(2-\nu_g)$ with μ_g and ν_g being the shear modulus and Poisson ratio of grain material (glass for this experiment), respectively; $\phi = \rho/\rho_{glass}$ is the packing fraction (ρ_{glass} is the density of glass): Z is the coordination number (averaged over grains). The EMT gives that the two constants in Eqs. (1) and (2) are

$$\gamma_0 = \sqrt{\frac{3-2\nu_g}{10-7\nu_g}}, \tag{7}$$

$$c_0 = \sqrt{\frac{C_n + \frac{3}{2}C_t}{20\pi\rho_{lp}}(\phi_{lp}Z_{lp})^{3/2}\left(\frac{6\pi P_{atm}}{C_n}\right)^{1/3}}, \tag{8}$$

and the density factor is

$$c_\rho^{EMT} = \sqrt{\left(\frac{\phi Z}{\phi_{lp}Z_{lp}}\right)^{3/2}\frac{\rho_{lp}}{\rho}}. \tag{9}$$

For further estimations,[14–17] we can take the coordinate number $Z = 2\sqrt{3}\phi/(1-\phi)$ and its value at the random loose pack $Z_{lp} = 4 = 2\sqrt{3}\phi_{lp}/(1-\phi_{lp})$. Parameters for glass are as follows: $\rho_{glass} = 2600$ kg/m^3, $\nu_g = 0.2$, and $\mu_g = 10$ GPa. This leads to $\rho_{lp} = 1.394$ g/cm^3, $\phi_{lp} = 53.6\%$, as well as the two constants $\gamma_0^{EMT} = 0.55$ and $c_0^{EMT} = 374$ m/s. Note that γ_0 predicted by EMT is smaller than our measured value (0.595). The density factor c_ρ^{EMT} is plotted in Fig. 5(a) (blue). There is

also another widely used empiric formula for it, suggested by Hardin and Richard[18]

$$c_\rho^{\mathrm{H-R}} = \frac{3.17-\rho_{\mathrm{glass}}/\rho}{3.17-\rho_{\mathrm{glass}}/\rho_{\mathrm{lp}}}, \tag{10}$$

see Fig. 5(a) (in black). Note that the two formulas (Eqs. (9) and (10)) give similar results. The correction of c_ρ to the sound velocity is not big, less than 15% for ρ varying from ρ_{lp} to ρ_{cp}. As in our experiment the density changes for both isotropic and uni-axial cases are small (<1.5%), we may conclude that influence of density change is negligible in our experiment.

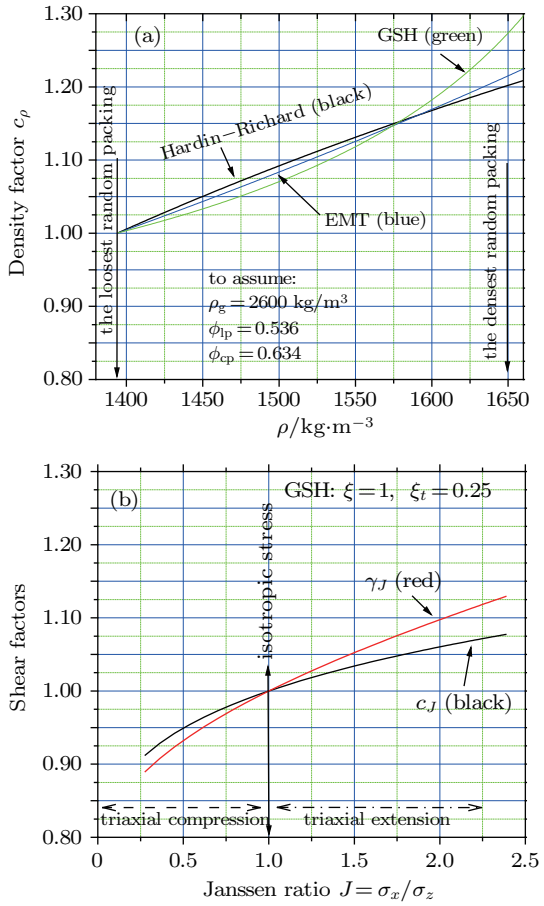


Fig. 5. (color online) (a) Density factors suggested by GSH, Hardin–Richard and EMT. (b) Two shear factors predicted by GSH. Parameters ξ and ξ_t are material parameters in the elastic potential of GSH (for details see Ref. [19]).

The two shear factors c_J and γ_J can be calculated with the elastic potential of GSH reported in Ref. [19], and the classical theory of elastic waves (see e.g., the textbook[20]). The results are plotted in Fig. 5(b), and the detailed expressions and derivations can be found in Ref. [19]. In the uni-axial experiment the Janssen ratio is usually considered to be less than 1 (typically $J \sim 0.7$), for which we have $c_J\gamma_J < 1$. Clearly neither of the behaviors of c_J and γ_J can be used for explaining our measured results, which shows that velocities for uni-axial case are greater than those in the isotropic stress case (see Figs. 2 and 4).

It is worth noting that the above discussion is limited to homogeneous and non-dissipative samples without boundary. However for understanding the experimental results, the modeling needs to go beyond the ideal situation, namely needs to consider effects due to existence of boundaries, the inhomogeneity of the sample, and the dissipation caused by the disturbance of the wave propagation in the future.

4. Conclusions and perspectives

In this study we experimentally investigate the pressure dependence of the sound velocity propagating in granular medium packed in a flexible and rigid wall container, with tri-axial and uni-axial devices respectively. Special attention is paid to the influences of repetitive loading-unloading stress cycles in a stress range 20 kPa–1000 kPa. We find that changes of the sound velocity with the number of stress cycles, as well as deviation from the Hertz 1/6-scaling law for its pressure dependence, cannot be explained by the influences of packing density nor Janssen ratio alone. Stress inhomogeneities, dissipations induced by sound wave propagation, and sample boundary conditions shall be the factors to be focused in our future studies.

References

[1] Timoshenko S and Goodier J N 1951 *Theory of Elasticity* (New York: McGraw-Hill Book Company, Inc.) p. 372
[2] Makse H A, Gland N, Johnson D L and Schwartz L M 1999 *Phys. Rev. Lett.* **83** 5070
[3] Makse H A, Gland N, Johnson D L and Schwartz L M 2004 *Phys. Rev. E.* **70** 061302
[4] Walton K 1987 *J. Mech. Phys. Solids* **35** 213
[5] Jia X, Caroli C and Velicky B 1999 *Phys. Rev. Lett.* **82** 1863
[6] Goddard J D 1990 *Proc. R. Soc. London A* **430** 105
[7] Hardin B O and Blandford G E 1989 *J. Geotech. Engng ASCE* **115** 788
[8] Khidas Y and Jia X 2010 *Phys. Rev. E* **81** 021303
[9] Jiang Y and Liu M 2015 *Eur. Phys. J. E* **38** 15
[10] Zhang Q, Li Y C, Hou M Y, Jiang Y M and Liu M 2012 *Phys. Rev. E* **85** 031306
[11] Zhang Z C and Cheng X H 2015 *Acta Geotechnica* **10** 781
[12] Goddard J D 1989 *Bull. Am. Phys. Soc.* **34** 822
[13] Digby P J 1981 *J. Appl. Mech. ASME* **48** 803
[14] Song C M, Wang P and Makse H A 2008 *Nature* **453** 629
[15] Wang Y J 2017 *Chin. Phys. B* **26** 014503
[16] Zhang X D, Xia C J, Xiao X H and Wang Y J 2014 *Chin. Phys. B* **23** 044501
[17] Xia C J, Li J D, Cao Y X, Kou B Q, Xiao X H, Fezzaa K, Xiao T Q and Wang Y J 2015 *Nat. Commun.* **6** 8409
[18] Hardin B O and Richart F E 1963 *J. Soil Mech. Found. Div. ASCE* **89** 33
[19] Jiang Y M, Zheng H P, Peng Z, Fu L P, Song S X, Sun Q C, Mayer M and Liu M 2012 *Phys. Rev. E* **85** 051304
[20] Landau L D and Lifshitz E M 1986 *Theory of Elasticity*, 3rd edn. (New York: Pergamon Press)